Journal of Structural Geology, Vol. 14, No. 1, pp. 11 to 17, 1992
Printed in Great Britain

0191-8141/92 $05.00+0.00
Pergamon Press plc

Estimated obliquities between the horizontal traces of *X–Y* surfaces and foliation trajectories in strained orthogneiss

W. M. SCHWERDTNER and E. J. COWAN

Department of Geology, University of Toronto, Toronto, Ontario, Canada M5S 3B1

(*Received* 22 *May* 1990; *accepted in revised form* 30 *May* 1991)

Abstract—The geometrical style of mineral foliation varies greatly within deformed metaplutonic masses, and the angle between foliation trajectories and horizontal traces of *X–Y* surfaces of total strain depends largely on this variation. In laminated orthogneiss derived from protoliths with isolated megacrysts or polycrystalline aggregates, the foliation trajectories can be markedly oblique to the traces of the *X–Y* surface. The obliquity angle (δ) depends on (1) the boundary migration of mineral aggregates, (2) the finite strain accumulated during the production of laminae and (3) the finite deformation imposed on laminated gneiss. Prediction of the obliquity angle is difficult because (1) and (2) are effectively unknown, and (3) varies greatly with position. By assuming that (i) all isolated aggregates behave as if they deform coaxially while being transformed into laminae and (ii) all laminae rotate as passive markers, we were able to calculate the obliquity angle for a range of laminae-producing strains and a spectrum of imposed plane deformations. These results apply to rocks located on the symmetry planes of large folds and *X–Z* sections of shear zones. Here the obliquity between foliation trajectory and the horizontal trace of *X–Y* plane is <15°, for any amount of laminae-deforming strain, if the formation of laminae requires horizontal strain ratios of >2.4. Even if the laminae-producing strain is as low as 2.0, $\delta < 15°$ provided that the ratio of laminae-deforming strain is <1.8. Higher strain ratios may be ruled out if the laminae are effectively planar, on the scales of centimetres to metres, or where the short limbs of open buckles in gneissosity resemble conjugate kink bands or chevron folds.

INTRODUCTION

PRINCIPAL *strain* trajectories are valuable tools in studying the deformation pattern of large-scale structures (Hossack 1978, Cobbold 1979), but such trajectories can rarely be mapped in three dimensions. *Foliation* trajectories, on the other hand, appear on many structural maps, and are regarded as effectively parallel to the horizontal traces of *X–Y* surfaces of total strain (Brun & Pons 1981, Brun *et al.* 1981, Andrews *et al.* 1986, Paterson & Tobisch 1988, Schwerdtner 1990). This practice is problematic where foliation comprises mineral laminae which are coplanar, or disrupted by shear bands, or thrown into buckle folds (Fig. 1). Even if laminae deform in a passive manner they cannot remain pegged to the *X–Y* plane of non-coaxial strain (Schwerdtner 1973, Le Theoff 1979, Suppe 1985, p. 98).

The scale at which foliation may be viewed as planar is generally an order of magnitude larger than the wavelength of small folds or spacing of narrow bands. On that scale, the obliquity between foliation trajectories and horizontal traces of *X–Y* surfaces may greatly change with position.

This paper summarizes the results of two-dimensional geometrical studies in which we estimate the final angle δ between the mineral-aggregate lineation (foliation trace) and the direction of maximum total extension (Fig. 2). In our study, δ depends on two states of finite pure shear: a first strain which creates a set of laminae and a second strain which deforms the laminae. These pure shears represent the distortion components of natural non-coaxial deformations.

DEVELOPMENT OF STRINGERS OR LAMINAE: FIRST STRAIN

Many gabbroid and granitoid rocks contain subequant xenoliths and isolated mineral constituents such as mafic igneous clots or felsic igneous megacrysts (Ramsay & Graham 1970, Ramsay 1989). Metamorphic derivatives of such primary inclusions become highly inequant and assume preferred orientations as the rocks are transformed into orthogneiss (Ramsay & Huber 1983, pp. 36, 46, 1987, p. 590). Transitions between subellipsoidal mineral aggregates and polycrystalline laminae may be observed within individual orthogneiss units (Davidson 1983, Schwerdtner 1988, 1990). Where rocks have been stretched rather than flattened, cigar-shaped mineral aggregates grade into very long stringers over distances of a few metres or tens of metres. Such stringers have subcircular cross-sections in which the apparent distortion of the aggregate boundaries is very much smaller than that in longitudinal section.

Many stringers are considerably larger than their weakly strained parents. For example, mafic stringers in stretched anothositic sheets of the western Grenville Province (Van Kranendonk 1985) have minimum volumes which are two orders of magnitude larger than the average volume of subequant mafic clots found at dis-

tances of <50 m along strike. This suggests that clot boundaries migrate and eventually coalesce during deformation (Robin 1979, Sawyer & Robin 1986). Aggregate boundaries are predicted to migrate in such a way that they *shrink* in the direction of maximum instantaneous shortening and *grow* in the direction of maximum instantaneous extension. This process combines with non-coaxial passive deformation and promotes coalescence of aggregates in the lineation direction.

Consider an elliptical mafic clot that has aligned itself with the direction of early principal extension, by the combined effects of passive deformation and boundary migration, and has become representative of the aggregate-shape fabric (Fig. 3a). The diameter ratio of the strain ellipse is smaller than that of the shape fabric ellipse, therefore subsequent passive deformation reorientates the progressive strain ellipse at a faster rate than the shape ellipse (Schwerdtner 1973, Le Theoff 1979). Passive deformation would result in an obliquity (ω) with counter-clockwise sense, between the major diameters of progressive strain and passively deformed shapes of mineral aggregates (Fig. 3b). Boundary migration, on the other hand, increases the clot length in the direction of maximum instantaneous extension, at an angle ρ to the major diameter of the progressive strain ellipse (Fig. 3b). Angles ω and ρ differ greatly in absolute magnitude for some types of non-coaxial strain, but their sense is always opposite. This justifies the simple assumption that the combined effect of passive deformation and boundary migration keeps the fabric ellipse coaxial with the progressive strain ellipse until the rocks possess coplanar laminae or colinear stringers.

The magnitude of the first finite strain is unknown, but probably depends on rock type and physical condition of ductile deformation. We decided to vary the hypothetical magnitude of first finite shortening from 10 to 70%, which corresponds to strain ratios of 1.2 and 11.1, respectively (Figs. 2, 4 and 5).

DEFORMATION OF STRINGERS AND LAMINAE: SECOND STRAIN

In spite of *non-coaxial* isochoric rock strain (Fig. 3), coalescing mineral aggregates are assumed to behave as if they deform *coaxially*. Unlike isolated mineral aggregates, gneissic laminae and stringers will rotate, but not necessarily strain, as if they are passive markers (Fig. 2). If $0° < \theta < 90°$ (Figs. 2, 4 and 5), the principal directions of progressive strain will deviate from the stringer direction and lamination normal. However, the final orientation of passive laminae and stringers will be independent of the deformation path and completely determined by the principal ratios of the first and second strains, together with the angle of superposition θ (see Fig. 2, and the Appendix). Accordingly, all unmarked points on the curves in Figs. 4 and 5 represent final geometric states rather than stages of progressive deformation.

The path-independence of the curves is exemplified for simple shearing, even though it may be rare in natural structures (De Paor 1987). The end of the simple-shear path may be seen by using the simple-shear scale in Figs. 4 and 5, whereby the orientation of the shear plane varies with magnitude of γ (finite unit shear) as specified in Fig. 6 and the Appendix.

OBLIQUITY ANGLES (δ) IN PLANE STRAIN

Large δ-angles are obtained if $\theta < 30°$ and the first shortening is 10–30% (Fig. 4). However, small θ angles can probably be ruled out where the laminae have escaped late-stage buckling. Moreover first-shortening values of <35% or strain ratios <2.4 seem unrealistic in comparison to those of well-studied metaplutonic rocks that are devoid of laminae. For example Ramsay & Huber (1983, pp. 81 and 86) obtained a ratio of 2.6 in weakly foliated xenolith-rich granite that lacks evidence of marked aggregate boundary migration. For first strain ratios of >2.4, maximum δ-values are about 15° (Figs. 4 and 5). The application of this result is not restricted to plane deformations because strain ratios are independent of area change.

Even if $\theta < 30°$ and the first strain is as low as 2.0, δ remains <15° so long as the second strain ratio does not exceed 1.8, i.e. 25% shortening in pure shear (Fig. 4b). These conditions probably hold in kinked or gently crenulated orthogneiss where the ductile thickening of laminae is negligible (Paterson & Weiss 1966, Cobbold & Gapais 1986, Ramsay & Huber 1987, p. 415).

The results of the preceding geometrical study are directly applicable to metaplutonic masses that have been deformed by heterogeneous transcurrent shear (Ramsay & Graham 1970, Berthé *et al.* 1979). Such masses are characterized by horizontal mineral lineation and vertical foliation, so that the foliation trajectories coincide with the lineation trajectories and the prolateness factor (Flinn 1962) of the total strain ellipsoid does not depart from unity (Schwerdtner *et al.* 1977). A regional component of vertical extension, e.g. in transpression zones (Sanderson & Marchini 1984), lowers the k-value everywhere and causes a loss in horizontal area even if the triaxial total strain is isochoric. Such area loss alters the shortening percentages in Figs. 4 and 5, but does not affect the angular relationship discussed in the previous paragraphs. The strain ratios shown in Figs. 4 and 5 apply also to any orthogneiss located on symmetry planes of large-scale deformation fields (Schwerdtner 1988), e.g. traces of vertical hinge planes in upright orthorhombic folds or traverses across ductile thrusts.

A difficulty arises where symmetry planes of large structures are strongly inclined. At any locality on the trace of such symmetry planes, the horizontal surface is an arbitrary section through the general ellipsoid of triaxial total strain. This implies that the major diameter of the section ellipse is oblique to the horizontal trace of the X–Y plane (Flinn 1962, Ramsay 1967, p. 160). The angle between this horizontal diameter and the X–Y plane varies with shape and orientation of the total-

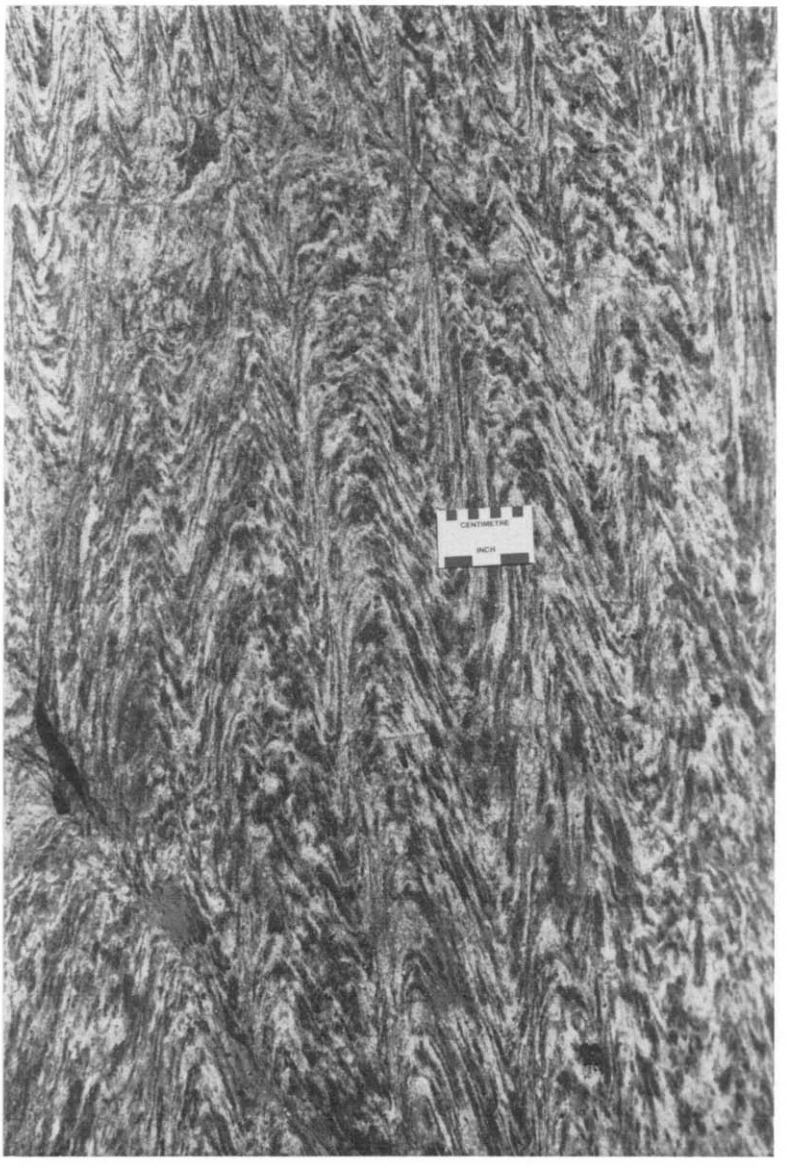

Fig. 1. Gentle buckling of the foliation in a metatonalite on Highway 69, west of Gibson Lake, central Ontario (Schwerdtner & Mawer 1982, fig. 26.2). The fold axis makes an angle of $<10°$ with the outcrop surface, which exaggerates the fold amplitude and therefore facilitates the identification of the gentle buckles.

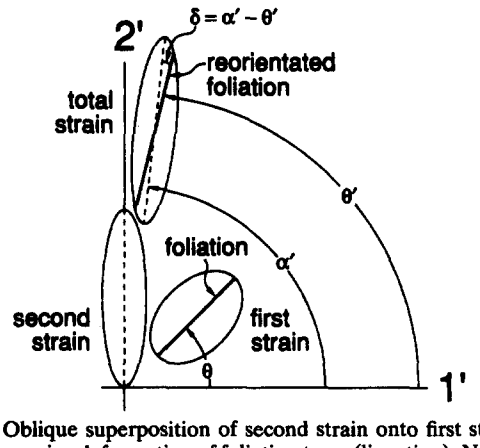

Fig. 2. Oblique superposition of second strain onto first strain, and ensuing passive deformation of foliation trace (lineation). Note angles used in the mathematical equations (see the Appendix) and throughout the text.

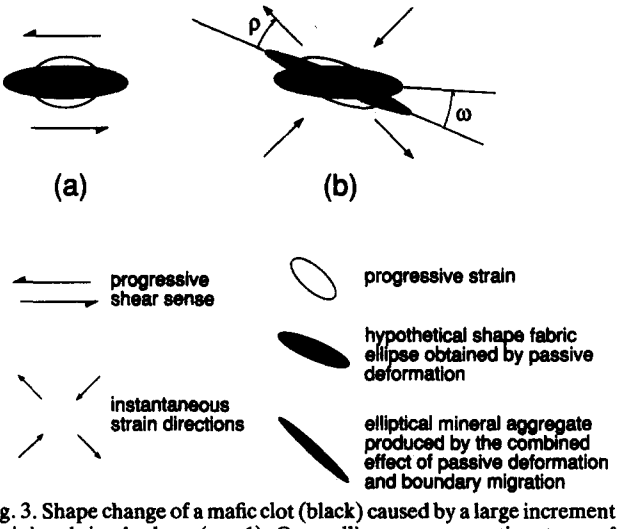

Fig. 3. Shape change of a mafic clot (black) caused by a large increment of sinistral simple shear ($\gamma = 1$). Open ellipses = consecutive stages of progressive strain (a & b), prior to coalescence and cessation of first strain. Note that ρ and ω have opposite sense, and that the clot is assumed to remain parallel to the strain ellipse.

strain ellipsoid, which are generally unknown. This precludes the use of Figs. 4 and 5, in which δ is measured with respect to the major diameter of the horizontal strain ellipse (Fig. 2), rather than the trace of the X–Y plane.

CONCLUSIONS

Many orthogneiss masses contain rocks with coplanar laminae produced by severe strain and synkinematic coalescence of spaced mineral aggregates (recrystallized igneous megacrysts, etc.). In such rocks, foliation trajectories can be markedly oblique to the horizontal traces of X–Y surfaces of total strain, and field geologists need to know where this obliquity is largest.

We made crude estimates of the obliquity angle (δ) which apply to rocks located on effective-symmetry planes of total-strain fields. Such symmetry planes may coincide with the peneplain across upright vertical folds or transcurrent shear zones. Structures such as canoe-

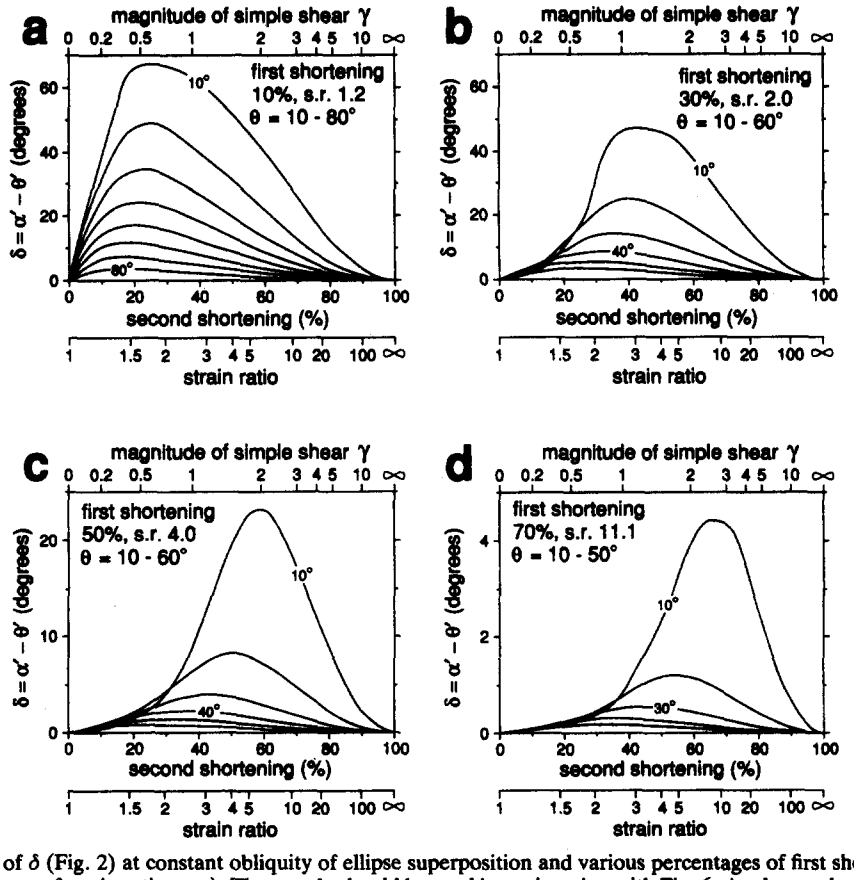

Fig. 4. Values of δ (Fig. 2) at constant obliquity of ellipse superposition and various percentages of first shortening (also expressed in terms of strain ratios s.r.). The γ-scale should be used in conjunction with Fig. 6. Angles used are indicated in Fig. 2.

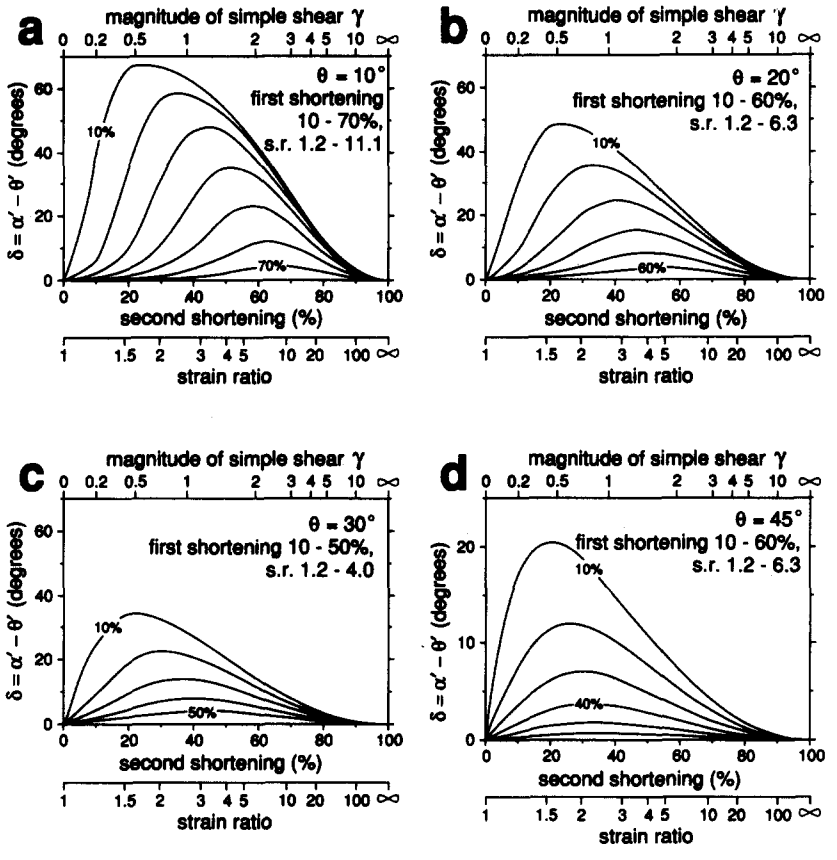

Fig. 5. Values of δ (Fig. 2) at constant percentage of first shortening or strain ratio (s.r.). The γ-scale should be used in conjunction with Fig. 6. Angles used are indicated in Fig. 2.

shaped synclines or parallel-sided zones of thrust shear have vertical symmetry planes whose horizontal traces may also be analysed by using Figs. 4 and 5. Here $\delta < 15°$ if the formation of laminae requires horizontal strain ratios of >2.4, for any amount of laminae-deforming strain. Even if the laminae-producing strain is as low as 2.0, $\delta < 15°$ provided that the ratio of laminae-deforming strain is <1.8. Higher strain ratios are generally indicated by close buckles or microlithons in the foliation, which may be identified in the field.

Schistosity becomes conspicuous at a strain ratio of 2.1 (Ramsay 1967, p. 180), but field geologists feel that the laminae-producing strain ratio in orthogneiss is >2.4. If this intuition proves correct and our assumptions are valid then the obliquity between the foliation trajectory and horizontal trace of X–Y plane should be less than 15°, provided that the foliation is not closely folded on the scales of centimetres or decimetres.

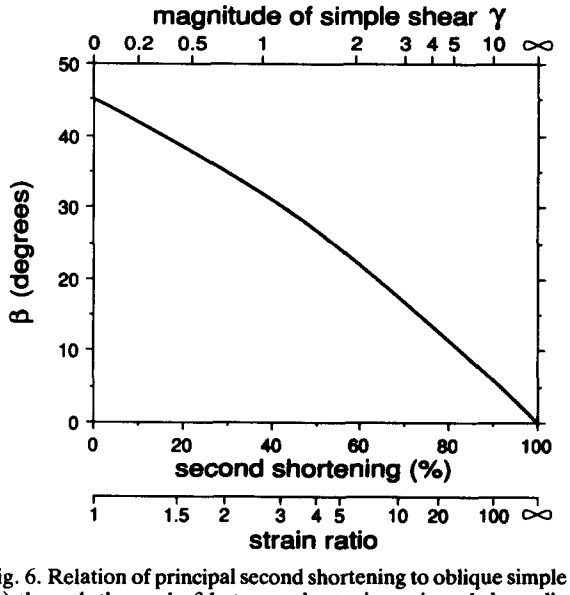

Fig. 6. Relation of principal second shortening to oblique simple shear (γ) through the angle β between shortening axis and shear direction (equation A3, see Appendix).

Acknowledgements—This work was supported by the National Research Council of Canada and the Ontario Geological Survey. The authors are indebted to Pierre-Yves Robin, Howard Williams, Win Means, Scott Paterson, Graham Borradaile, Declan De Paor and Bill Shanks for reading different versions of the paper and/or offering valuable advice. Donna Kong is thanked for typing the manuscript.

REFERENCES

Andrews, A. J., Hugon, H., Durocher, M., Corfu, F. & Lavigne, M. J. 1986. The anatomy of a gold-bearing greenstone belt: Red Lake, northwestern Ontario, Canada. In: *Gold '86 Proceedings Volume* (edited by Macdonald, A. J.), Toronto, 3–22.

Berthé, D., Choukroune, P. & Jegouzo, P. 1979. Orthogneiss, mylonite and non coaxial deformation of granites: the example of the South Armorican Shear Zone. *J. Struct. Geol.* **1**, 31–42.

Brun, J. P., Gapais, D. & Le Theoff, B. 1981. The mantled gneiss domes of Kuopio (Finland): interfering diapirs. *Tectonophysics* **74**, 383–404.

Brun, J. P. & Pons, J. 1981. Strain patterns of pluton emplacement in a crust undergoing non-coaxial deformation. *J. Struct. Geol.* **3**, 219–229.

Cobbold, P. R. 1979. Removal of finite deformation using strain trajectories. *J. Struct. Geol.* **1**, 67–72.
Cobbold, P. R. & Gapais, D. 1986. Slip system domains. I. Plane strain kinematics of arrays of coherent bands with twinned fibre orientations. *Tectonophysics* **131**, 113–132.
Davidson, D. M. 1983. Strain analysis of deformed granitic rocks (Helician), Muskoka district, Ontario. *J. Struct. Geol.* **5**, 181–195.
De Paor, D. G. 1987. Stretch in shear zones: implication for section balancing. *J. Struct. Geol.* **9**, 893–895.
Flinn, D. 1962. On folding during three-dimensional progressive deformation. *Q. J. geol. Soc. Lond.* **118**, 385–433.
Hossack, J. R. 1978. The correction of stratigraphic sections for tectonic finite strain in the Bygdin area, Norway. *J. geol. Soc. Lond.* **135**, 229–241.
Jaeger, J. C. 1962. *Elasticity, Fracture and Flow* (2nd edn). Methuen, London.
Le Theoff, B. 1979. Noncoaxial deformation of elliptical particles. *Tectonophysics* **53**, T7–T13.
Nye, J. F. 1960. *Physical Properties of Crystals*. Oxford University Press, London.
Paterson, M. S. & Weiss, L. E. 1966. Experimental deformation and folding in phyllite. *Bull. geol. Soc. Am.* **77**, 343–374.
Paterson, S. R. & Tobisch, O. T. 1988. Using pluton ages to date regional deformations: problems with commonly used criteria. *Geology* **16**, 1108–1111.
Ramsay, J. G. 1967. *Folding and Fracturing of Rocks*. McGraw-Hill, New York.
Ramsay, J. G. 1989. Emplacement kinematics of a granite diapir: the Chindamora batholith, Zimbabwe. *J. Struct. Geol.* **11**, 191–209.
Ramsay, J. G. & Graham, R. H. 1970. Strain variation in shear belts. *Can. J. Earth Sci.* **7**, 786–813.
Ramsay, J. G. & Huber, M. I. 1983. *The Techniques of Modern Structural Geology, Volume* 1: *Strain Analysis*. Academic Press, London.
Ramsay, J. G. & Huber, M. I. 1987. *The Techniques of Modern Structural Geology, Volume* 2: *Folds and Fractures*. Academic Press, London.
Robin, P.-Y. F. 1979. Theory of metamorphic segregation and related processes. *Geochem. cosmochim. Acta.* **43**, 1587–1600.
Sanderson, D. J. & Marchini, W. R. D. 1984. Transpression. *J. Struct. Geol.* **6**, 449–458.
Sawyer, E. W. & Robin, P.-Y. F. 1986. The subsolidus segregation of layer-parallel quartz–feldspar veins in greenschist to upper amphibolite facies metasediments. *J. metamorph. Geol.* **4**, 237–260.
Schwerdtner, W. M. 1973. Schistosity and penetrative mineral lineation as indicators of paleostrain directions. *Can. J. Earth Sci.* **10**, 1233–1243.
Schwerdtner, W. M. 1988. Recognition of pervasive prestrain in the total-strain pattern of large folds. *J. Struct. Geol.* **10**, 33–40.
Schwerdtner, W. M. 1990. Structural tests of diapir hypotheses in Archean crust of Ontario. *Can. J. Earth Sci.* **27**, 387–402.
Schwerdtner, W. M., Bennett, P. J. & Janes, T. W. 1977. Application of L–S fabric scheme to structural mapping and paleostrain analysis. *Can. J. Earth Sci.* **14**, 1021–1032.
Schwerdtner, W. M. & Mawer, C. K. 1982. Geology of the Gravenhurst region, Grenville Structural Province, Ontario. *Geol. Surv. Pap. Can.* **82-1B**, 195–207.
Suppe, J. 1985. *Principles of Structural Geology*. Prentice-Hall, Englewood Cliffs, New Jersey.
Van Kranendonk, M. 1985. Anorthosite studies: Muskoka District, Haliburton and Victoria Counties. *Ontario geol. Surv. Misc. Pap.* **126**, 127–130.

APPENDIX: STRAIN CALCULATIONS

As shown in Fig. 2, we derived the plots of Figs. 4–6 by using the components of the total-deformation tensor (D_{ij}) expressed in suffix notation (Nye 1960). In a biaxial frame of reference, the first-strain ellipse makes an angle of θ with axis 1′ and the second-strain ellipse is parallel to axis 2′ (Fig. 2). Therefore, A'_{ij} are non-principal components of the first strain and

$$(D'_{ij}) = \begin{pmatrix} A'_{11}B'_{11} & A'_{12}B'_{11} \\ A'_{12}B'_{11} & A'_{22}B'_{11} \end{pmatrix}, \tag{A1}$$

where $i, j, m = 1, 2$ and $A_{22} = 1/A_{11}$ and $A'_{12} = A'_{21}$ and B'_{11} is the minor radius of the second-strain ellipse.

Moreover,

$$A'_{ij} = l_{im}l_{jm}A_{mm}, \tag{A2}$$

where direction cosines

$$(l_{ij}) = \begin{pmatrix} \cos\theta & \sin\theta \\ -\sin\theta & \cos\theta \end{pmatrix}.$$

The magnitude of simple shear

$$\gamma = -B'_{11} + 1/B'_{11}, \tag{A3}$$

which differs in sign from Jaeger's (1962, p. 33) expression because our axis 1′ is the maximum shortening direction (Fig. 2). The calculation of α', θ' and β in terms of (D'_{ij}) was done using equations by Jaeger (1962, pp. 24–33), and denoting the angle between the shear direction and axis 1′ as β.